Thickness-Lamé Thin-Film Piezoelectric-on-Silicon Resonators

Sarah Shahraini, *Student Member, IEEE*, Hakhamanesh Mansoorzare, *Graduate Student Member, IEEE*, Amirreza Mahigir, *Student Member, IEEE*, and Reza Abdolvand, *Senior Member, IEEE*

***Abstract*— In this paper, Thickness-Lamé (TL) mode piezoelectrically-transduced silicon resonators are studied and demonstrated. It will be shown that unlike Planar-Lamé resonance modes, Thickness-Lamé modes could be efficiently excited using sputtered polycrystalline piezoelectric films such as Scandium Aluminum Nitride (ScAlN) due to the constructive contribution of both d_{31} and d_{33} piezoelectric coefficients in the coupling coefficient. Moreover, it is shown through finite element analysis and experimental results that the coupling coefficient improves with the order of the TL harmonic mode excited in a silicon slab. It is also confirmed that the quality-factor of TL resonators substantially enhances through utilization of properly-designed acoustic reflectors (i.e. acoustic isolation frames) around the tethered resonator block. The temperature coefficient of frequency is also modeled using finite-element eigen-frequency analysis. It is shown that the turnover temperature of TL resonators aligned to the [100] plane of a degenerately-doped n-type silicon substrate varies considerably as the mode shape transitions from a Thickness-Lamé to a Lateral-Extensional mode with the gradual increase of wavelength to thickness ratio. A record Q of 23.2k is measured for a ∼185MHz fundamental TL resonator in vacuum ($f \times Q = 4.3 \times 10^{12}$) while quality factors of 12.6k ($f \times Q = 4.6 \times 10^{12}$) and 6k are also measured in vacuum for second- and third-harmonic TL resonators at 326 MHz and 555 MHz respectively. The combination of high turnover temperatures (>80 °C), high quality factor, and low motional resistance, promises the suitability of such resonators for extremely-stable oven-controlled oscillator applications. [2019-0263]**

***Index Terms*— AlN resonator, coupling efficiency, Lamé mode, microelectromechanical systems, quality factor optimization, turnover temperature tuning.**

I. Introduction

MICRO electro-mechanical resonators are at the heart of integrated low-noise oscillators, filters and sensors [1]–[5]. High quality factor (Q) and large coupling efficiency combined with high thermal stability and power handling in small form factors are desired for such applications. Although MEMS resonators offer high quality factor and coupling efficiency in small size, they generally suffer from relatively high temperature coefficient of frequency (TCF). The temperature coefficient of elasticity (TCE) is around −60 ppm/°C (TCF∼ −30 ppm/°C) for lightly-doped silicon based MEMS resonators [6], around −50 ppm/°C (TCF∼ −25 ppm/°C) for AlN based resonators [7] and around −140 to −180 ppm/°C (TCF∼ −70 ppm/°C to −90 ppm/°C) for Lithium Niobate (LN) resonators [8]. The reported high TCF for MEMS resonators limits their usage in ultra-stable oscillator applications.

Active and passive temperature compensation methods have been studied to reduce the temperature-induced frequency drift. Degenerate doping of the silicon device layer [9], or incorporation of a material with positive TCE (such as silicon dioxide) in the form of over-layers [3] or pillars [10] within the resonant structure are amongst the proposed passive temperature compensation methods. However, using an over-layer of oxide adversely impacts both the quality factor (partially due to energy scattering between layers) and the coupling efficiency while adding to the fabrication complexity. With passive temperature compensation of MEMS resonators, sub-ppm temperature stability remains out of reach, even though required for many ultra-stable clock applications.

In active temperature compensation methods on the other hand, the resonance frequency is actively tuned in real-time to compensate for the frequency drift caused by the ambient temperature variations. The most widely studied methods for active temperature compensation are tuning the termination impedance [11], [12], inducing a variable mechanical stress [13] and operating the resonator at a constant elevated temperature [14] (e.g. oven controlled oscillators). With active temperature compensation methods sub ppm temperature stability could be achieved over the desired temperature range. Oven controlled quartz crystal oscillators (OCXO) have been widely studied in the literature [15] and the same approach could be used for temperature compensation in MEMS resonators. However, this requires for the resonator turnover temperature (the temperature at which the TCF changes polarity) to be greater than the highest nominal operation range. This is because the TCF is virtually zero at turnover temperature and therefore the oscillator stability would be only marginally affected by the temperature control circuitry. Hence, designing resonators with turnover temperature values

Manuscript received December 16, 2019; revised January 23, 2020; accepted February 2, 2020. Date of publication March 12, 2020; date of current version June 2, 2020. This work was supported in part by the National Science Foundation (NSF) under Award 1711632. Subject Editor S. Gong. *(Corresponding author: Sarah Shahraini.)*

Sarah Shahraini and Amirreza Mahigir are with the Department of Electrical and Computer Engineering, University of Central Florida, Orlando, FL 32816 USA (e-mail: sarah.shahraini@knights.ucf.edu).

Hakhamanesh Mansoorzare is with the Department of Electrical and Computer Engineering, University of Central Florida College of Engineering and Computer Science, Orlando, FL 32816 USA.

Reza Abdolvand is with the Department of Electrical and Computer Engineering, University of Central Florida, Orlando, FL 32816 USA.

Color versions of one or more of the figures in this article are available online at http://ieeexplore.ieee.org.

Digital Object Identifier 10.1109/JMEMS.2020.2972779

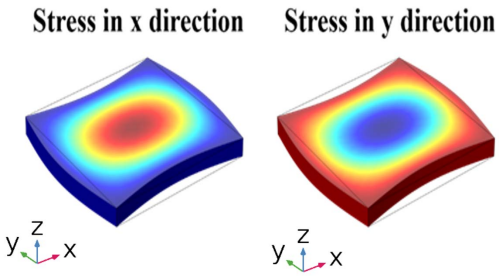

Fig. 1. The simulated stress field in the x and y directions for a pure AlN planar Lamé mode. In each half vibration cycle, stress field is tensile in one planar axis and compressive in the other axis (dark blue and dark red indicate maximum opposing stresses in the center). Therefore, such a planar Lamé mode cannot be efficiently excited with thin polycrystalline films laid on top of the resonator body.

above the commercial operation range (80 °C) is critical in realizing oven-controlled oscillators.

Based on the results reported in literature [6], Lamé mode silicon resonators exhibit the highest turnover temperature amongst conventional resonance modes for a given silicon doping concentration.

Although capacitive excitation of planar Lamé modes is frequently reported in silicon resonators at MHz regime [16], [17] but the motional resistance is usually large for these resonators especially at frequencies above 100MHz. Thin-film piezoelectric-on-substrate (TPoS) platform offers a pathway to reducing the motional resistance of high-Q silicon-based resonator. The substrate layer in a TPoS resonator (usually single crystalline silicon) concurrently enhances the power handling in these resonators as well [18].

That said, planar Lamé modes, cannot be efficiently actuated in silicon through piezoelectric transduction. This is because of the fact that the sputtered piezoelectric thin-films such as AlN are isotropic in the plane of the substrate. As illustrated in Fig. 1, the stress field is the same in magnitude but with opposite polarities in the X and Y directions for a planar Lamé mode and therefore charges cancel out on electrodes that are laid out across the thin film. In the case of piezoelectric on substrate resonators, since the symmetry would be disrupted with the presence of the substrate layer (i.e. silicon) planar Lamé modes could be actuated but the coupling efficiency would be extremely small (<0.0015%) which would drastically increase the motional resistance of the resonator [19], [20].

An alternative family of Lamé resonators coined as Cross-sectional Lamé mode resonators (CLMR) have been recently demonstrated in thin-film AlN resonators [21], [22] by exciting Lamé modes in the thickness of the AlN resonator. In CLMRs both d_{31} and d_{33} piezoelectric coefficients constructively contribute in the excitation of a two-dimensional mechanical vibration (excitation of the Lamé mode in the cross section of AlN film). As a result, these resonators offer coupling factors larger than what is achievable in lateral-extensional mode (also known as contour-mode) resonator. A possible limitation of such resonators is that the range of frequencies that could be achieved is relatively restricted to high frequencies. For lower-frequency designs the piezoelectric film thickness has to be in the range of 10s of micro-meter and processing such a thick piezoelectric film (i.e. deposition and etching) is not trivial if not practically impossible.

In this work we first demonstrate that Thickness-Lamé modes (TLM) could be efficiently excited in silicon with reasonably high Q using a thin-film piezoelectric sputtered on top of the substrate. Next, we will propose an acoustic isolation technique to effectively alleviate support loss for the TLM resonators implemented in the thin-film ScAlN-on-silicon (TPoS) platform. Next, temperature frequency dependency is modeled and studied for TLM TPoS resonators on a highly-doped n-type silicon layer using COMSOL. Our simulations confirm that turnover temperature of above 100 °C is achievable for these resonators at moderately high-doping concentrations ($\sim 4\times 10^{19}$ /cm^3). Next, using the COMSOL model and experimental results, we show that the turnover temperature is tunable by changing the resonator effective width to the thickness ratio as the targeted mode transitions from a Lamé to a quasi Lamé mode and finally converges to lateral-extensional modes. It will also be shown that higher harmonics of the TLM could be excited in the same silicon resonator slab. In fact, the coupling factor for the harmonic TLM resonators increases with the harmonic order.

II. Thickness-Lame Mode in TPoS Resonators

Commonly, the d_{31} piezoelectric coefficient of sputtered piezoelectric films (e.g. AlN) is utilized to excite lateral-extensional (LE) modes in TPoS resonators. For the fundamental LE mode, the width of the resonator is equal to resonance half-wavelength. To actuate higher harmonics, interdigitated electrode patterns are used. In such patterns the distance between the centers of two adjacent electrodes (also known as the finger-pitch (FP)) is equal to the half-wavelength.

As shown in Fig. 2.a, a pure lateral-extensional mode is actuated in a silicon slab when the half-wavelength ($\lambda/2$) $\gg$ thickness (Th). As $\lambda/2$ (i.e. width (W)) decreases and approaches the thickness of the resonator, mode shapes with properties between lateral-extensional mode and Lamé mode emerge in the thickness of the resonator (Fig. 2.b and Fig. 2.c). Eventually, when $\lambda/2$=Th, a pure Thickness-Lamé mode would be actuated in the resonator slab (Fig. 2.d).

Now, if a thin piezoelectric film sandwiched between two metal layers is laid out on top of the silicon slab as is the case in TPoS platform, the d_{31} and d_{33} piezoelectric coefficients of the film, constructively contribute in actuating the Lamé-mode in the composite structure of (Mo/AlN/Mo/Si). Caused by the presence of the piezoelectric film and metal layers, the symmetry of the acoustic medium is perturbed and therefore technically speaking a pure Lamé-mode can no longer be excited. Therefore, we refer to these mode shapes as quasi thickness-lamé modes (QTLM). For QTLM resonators if the width or the FP is close to the thickness of the resonator, the resonator would have properties closer to the property of a pure Lamé mode resonator. As the FP increases the behavior of the resonator transitions from Lamé mode to the commonly excited lateral-extensional mode.

Harmonic QTLM could also be actuated in the thickness of the TPoS resonator. When the FP is chosen $\sim \frac{tickness}{n}$,

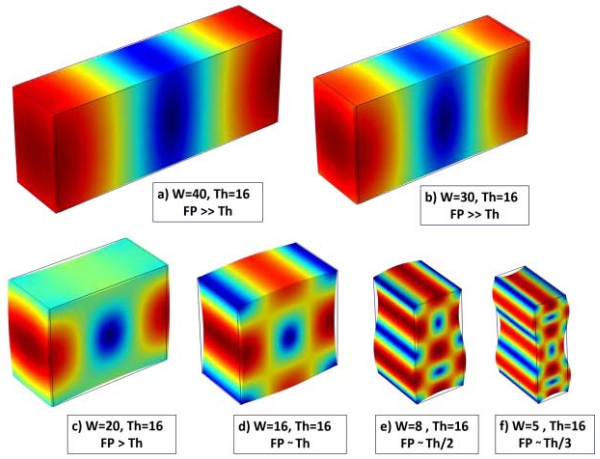

Fig. 2. The displacement field for a silicon block resonator with a thickness of Th=16μm and varying width (i.e. $\lambda/2$), where dark blue and dark red colors identify the minimum and maximum displacement respectfully. For the width values close to the thickness of the resonator, Lamé mode (d) would substitute lateral extensional mode (a) in the resonator slab. For the width values close to an integer fraction of the thickness of the resonator, higher harmonic thickness-Lamé modes are actuated in the resonator slab (e.g. second harmonic (e) and third harmonic (f)).

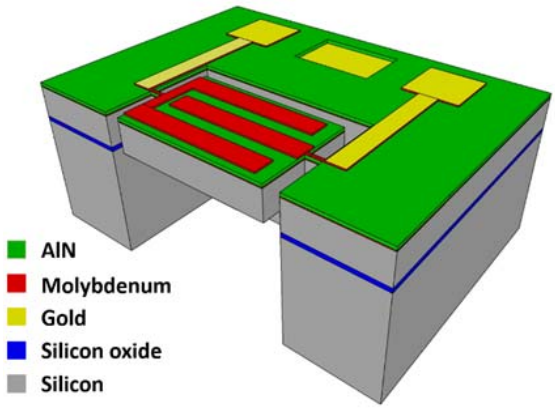

Fig. 3. A schematic viewgraph of a quasi-thickness-Lamé mode (QTLM) TPoS resonator. Electrode patterns are similar to the ones used for lateral extensional mode and the thickness of the silicon slab will enable excitation of the TL mode.

the nth harmonic in the thickness of the resonator is excited. For example, second and third harmonic QTLM are shown in Fig. 2.e and Fig. 2.f. Actuating higher order harmonics in the thickness of the resonator extends the range of frequencies that could be achieved on the same substrate with QTLM resonators.

A schematic viewgraph of a QTLM TPoS resonator is shown in Fig. 3. Based on the FP/Th ratio the same structure enables actuation of the lateral-extensional and the thickness quasi Lamé modes.

III. Quasi Lame Mode TPoS Resonator Modeling

A. Coupling Efficiency for QTLM TPoS Resonators

As mentioned in the previous section, for the fundamental QTLM TPoS resonator, the stress field is concentrated in the center of resonator stack (mostly in the silicon). Therefore,

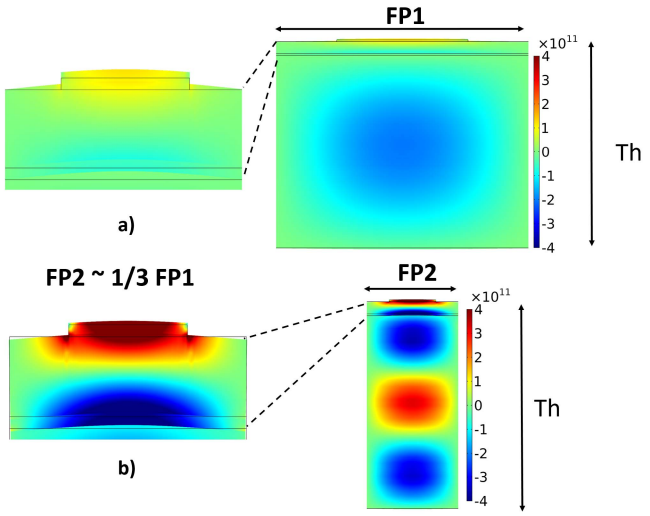

Fig. 4. The stress field in the fundamental a) and third harmonic b) QTLM resonators. The stress field in the piezoelectric portion of the third harmonic mode is larger and because of that higher coupling efficiencies are expected for third harmonic QTLM.

TABLE I

The Simulated Coupling Efficiencies for QTLM and LEM TPoS Resonators. A Full Stack of Mo/ScAlN/Mo/Si Is Considered With the Same Silicon Thickness as the Fabricated Resonators (0.1 μm Mo/1μm ScAlN/ 0.1μm Mo/ 16μm Si)

Mode shape	Silicon Thickness (μm)	20% ScAlN Thickness (μm)	Modeled K_t^2
Lateral-extensional	16	1	0.85%
1st harmonic QTLM	16	1	0.03%
2nd harmonic QTLM	16	1	0.08%
3rd harmonic QTLM	16	1	0.14%
Lateral-extensional	4	2	3.8%
2nd harmonic QTLM	4	2	7.8%

the stress concentration in the piezoelectric film is relatively small and the coupling efficiency is compromised. As higher order QTLM is actuated in the thickness of the resonator, the concentration of stress field within the piezoelectric region of the TPoS resonator increases (Fig. 4) and the coupling efficiency is expected to improve correspondingly.

A 2D loss-less frequency analysis model in COMSOL is used to study the coupling efficiency of the QTLM TPoS resonators. The resonator stack includes a 16μm silicon covered by 1μm thick ScAlN (20% Scandium content) sandwiched between two 100 nm Mo layers. The one port admittance is simulated using the frequency response analysis and the coupling efficiency is calculated using modeled series and parallel frequencies. The coupling coefficient for different harmonics are summarized in Table I. The material property information for 20% ScAlN is borrowed from [23].

As expected, the coupling efficiency increases for higher harmonic QTLM TPoS resonators and the QTLM will offer a

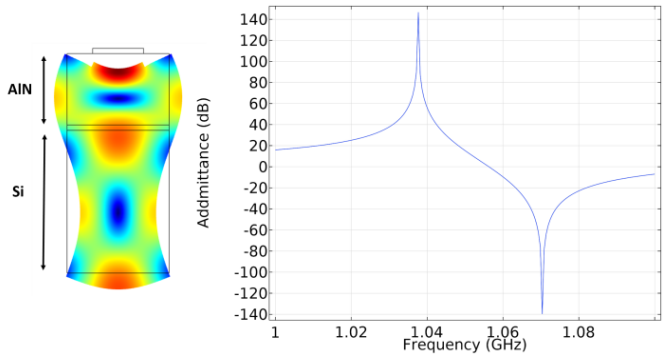

Fig. 5. The admittance modeled for a second-harmonic QTLM TPoS resonator with 4 μm silicon topped with 2μm ScAlN.

higher coupling factor than the lateral-extensional mode if the thickness of the piezoelectric film approaches half wavelength of the thickness Lamé mode.

A second-harmonic QTLM excited in a 4μm of silicon slab covered with a 2μm of piezoelectric film (20% ScAlN) is presented in Fig. 5. The simulated coupling factor is 7.8% for the second harmonic QTLM TPoS resonator.

B. Support Loss in QTLM TPoS *Resonators*

The resonator quality factor directly impacts the noise floor of the system in which the resonator is utilized. Therefore, achieving high quality factors are crucial for many applications such as oscillators and sensors. Anchor loss, ohmic loss and interface loss [24] are the main sources of loss in piezoelectric resonators. Although improving the interface loss might be challenging, these resonators can be designed for minimum anchor loss [25]–[27].

Since the Lamé mode in the QTLM TPoS resonators is formed on the cross-section of the resonator, there are no pseudo-nodal points at the sides of the resonator. Consequently, a substantial portion of acoustic energy could be radiated to the substrate through the tethers. By placing planar acoustic reflectors (etching trenches in the substrate), the acoustic wave is reflected due to the very large acoustic mismatch between air and silicon. If these reflectors are designed at the proper distance from the tether, the reflected wave would be constructively interfering with the resonator's standing wave [28]–[30].

In this work, we present a novel acoustic isolation frame to minimize the anchor loss for QTLM. As shown in Fig. 6, the resonator is carved out of a suspended circular frame. The radiated acoustic energy through tethers is reflected from the edges of this frame. Based on the size of the isolation frame the reflected acoustic energy could either improve or degrade the resonators quality factor. The anchor quality factor is optimized by optimizing the dimensions of the structure.

A 3D model based on a perfectly matched layer (PML) is developed in COMSOL to study the anchor loss for QTLM TPoS resonators. The dimension of the acoustic isolation frame is varied to search for the optimized frame dimensions. Based on the modeled data, the anchor quality factor is optimized when the acoustic isolation frame has a diameter

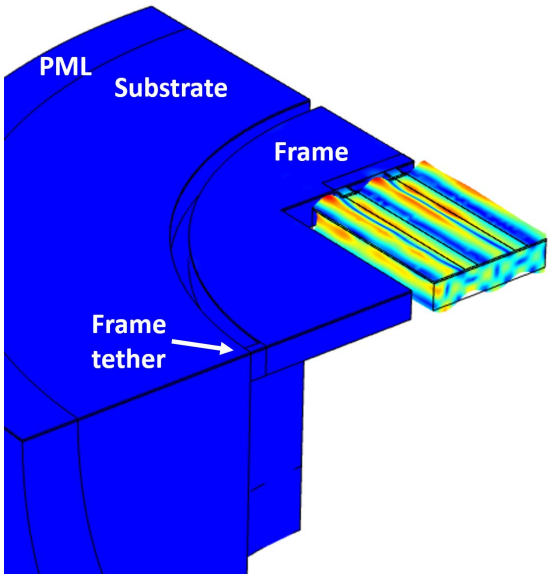

Fig. 6. The PML-based model developed for support loss prediction in a fundamental QTLM TPoS resonator with an acoustic isolation frame. The resonator and frame dimensions are chosen to resemble the fabricated resonators.

TABLE II
THE MODELED ANCHOR QUALITY FACTOR FOR THE RESONATOR WITH AND WITHOUT ACOUSTIC ISOLATION FRAME

Mode shape	Q_{anc} without isolation-frame	Q_{anc} With isolation-frame
1st harmonic QTLM TPoS	7.6 k	70 k

of (2n×FP/2) + 2 × (tether-length). The support quality factor is improved by an order of magnitude for the optimum frame dimensions (Table II) for the fundamental QTLM TPoS resonator with an FP= 17μm ($f_{resonance}$ ~185 MHz).

C. Turnover Temperature in QTLM TPoS *Resonators*

Lamé mode resonators in highly n-type doped silicon are excellent choices for oven-controlled oscillator applications for which, the oscillator operates at a constant elevated temperature. If this elevated temperature is close to the turnover temperature of the resonator, the system would be robust to the errors of the control system.

For [100] aligned QTLM TPoS resonator, all the resonator boundaries would be aligned to [100] crystalline plane of silicon Fig. 7. Therefore, it is expected that the temperature behavior of the [100]-aligned QTLM to be similar to planar Lamé modes fabricated on a 100 silicon substrate previously reported in [31].

To predict the frequency-shift as a function of the temperature for QTLM TPoS resonators, a 2-D model of the whole stack of TPoS resonators is developed in COMSOL. The layer thicknesses in the model reflect the fabricated devices as follows: top Molybdenum 100 nm, Scandium

TABLE III

THE ELASTIC CONSTANTS OF PHOSPHORUS-DOPED ($n = 6.6 \times 1019\ cm^{-3}$) SILICON AND THEIR CORRESPONDING FIRST AND SECOND ORDER TEMPERATURE COEFFICIENTS [6]

Dopant	C_{11} (GPa)	C_{12} (GPa)	C_{44} (GPa)	$T_{C_{11}}^{(1)}$ (ppm/°C)	$T_{C_{12}}^{(1)}$ (ppm/°C)	$T_{C_{44}}^{(1)}$ (ppm/°C)	$T_{C_{11}}^{(2)}$ (ppb/°C^2)	$T_{C_{12}}^{(2)}$ (ppb/°C^2)	$T_{C_{44}}^{(2)}$ (ppb/°C^2)
Phosphorus 6.6×10^{19}	164.0	66.7	78.2	-34.2	-135.2	-67.8	-103	-1	-40

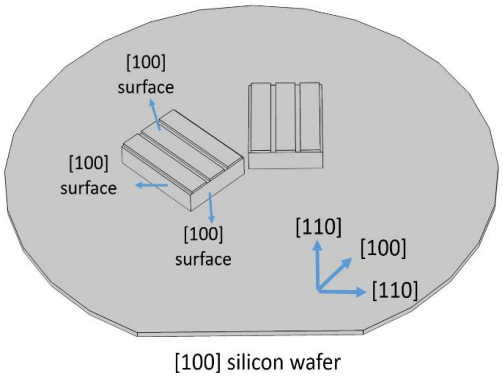

Fig. 7. On a [100] silicon wafer, the block resonators should be rotated 45 degrees with respect to the wafer flat in order for all faces to be aligned to [100] crystalline plane, which would be similar to the case for planar Lamé mode.

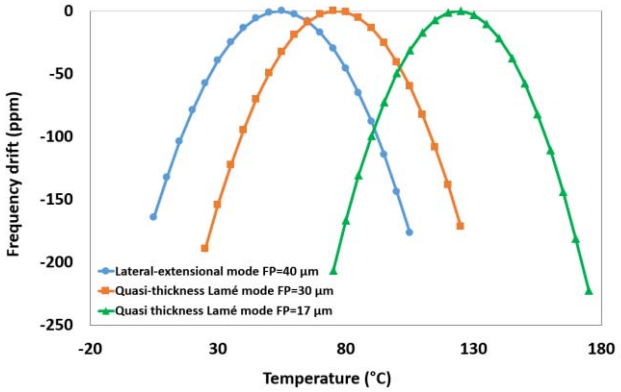

Fig. 8. The modeled TCF curves for resonators with FP 40, 30 and 17 μm. The turnover temperature shifts toward higher temperature as the FP/ T ratio approaches unity. The lateral-extensional mode exhibits the lowest turnover temperatures compared to QTLM resonators.

doped AlN (ScAlN) 1 μm, bottom Molybdenum 100 nm and silicon 16 μm.

In order to develop TCF curves, stiffness values for silicon, AlN and Molybdenum and their temperature coefficients were borrowed from [6](Table III) for phosphorus doped single crystalline silicon (n=$6.6\times10^{19}cm^{-3}$), [32] and [33] for AlN and Molybdenum respectively. The temperature coefficient of elasticity (TCE) of AlN is assumed to be an adequate replacement for Scandium doped AlN TCE data.

For single crystalline silicon, the stiffness matrix is calculated for each temperature using Eq.1, Eq.2 and Eq.3:

$$C_{11T} = C_{110} + TC_{11}^{1} \times C_{110} \times 10^{-6} \times (T - T_0) + TC_{11}^{2} \times C_{110} \times 10^{-9} \times (T - T_0)^2 \quad (1)$$

$$C_{12T} = C_{120} + TC_{12}^{1} \times C_{120} \times 10^{-6} \times (T - T_0) + TC_{12}^{2} \times C_{120} \times 10^{-9} \times (T - T_0)^2 \quad (2)$$

$$C_{44T} = C_{440} + TC_{44}^{1} \times C_{440} \times 10^{-6} \times (T - T_0) + TC_{44}^{2} \times C_{440} \times 10^{-9} \times (T - T_0)^2 \quad (3)$$

Where C_{11T}, C_{12T} and C_{44T} are the single crystalline silicon stiffness coefficients at an arbitrary temperature T referenced to the room temperature and C_{110}, C_{120} and C_{440} are the stiffness coefficient at room temperature (T_0).

The new stiffness matrix for silicon and stiffness values for ScAlN and Molybdenum are used to repeat the modal analysis and to calculate the shifted resonance frequency.

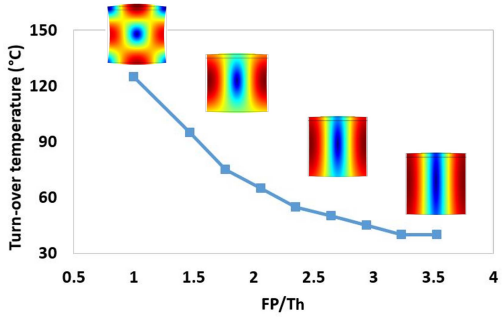

Fig. 9. The turnover temperature of a QTLM TPoS resonator as a function of FP/Th ratio. Higher turnover temperature is predicted for the resonators with FP/Th ratio closer to one. The turnover temperature could be adjusted lithographically.

The modeled TCF curves for TPoS resonators with FP of 40 μm, 30 μm and 17 μm are shown in Fig. 8. For the quasi thickness-Lamé mode resonators (FP=17 μm), it was expected that the resonator behavior would be similar to the pure Lamé mode which is confirmed with our model.

As the finger-pitch to thickness ratio increases the temperature-frequency behavior of the resonator transitions from what is known of pure Lamé to what is expected for extensional modes (i.e. the turnover temperature shifts down (Fig. 9).

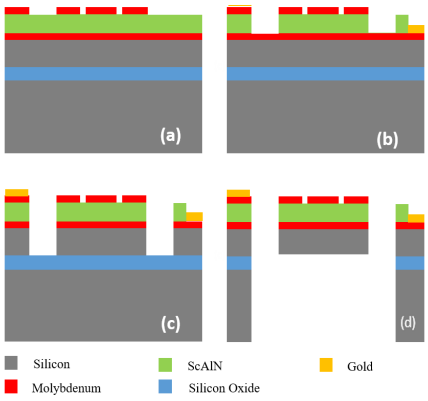

Fig. 10. The simplified schematic process flow for fabricating QTLM TPoS resonators.

Therefore, the turnover temperature in QTLM-TPoS resonators can be tuned lithographically by adjusting the FP/Th ratio. This feature can be used to design resonators with the turnover temperatures slightly above the desired temperature range for oven controlled oscillator application.

The TCF curves are also modeled for higher harmonics of QTLM TPoS resonator. For these higher order modes, the turnover temperatures are predicted to be slightly lower than the fundamental mode (turnover temperature = 120 °C). For the temperature range reported in this study, TCE is negative for both AlN and Molybdenum and positive for highly doped silicon. For the fundamental thickness-Lamé mode the stress filed is mostly concentrated in the center of the resonator (silicon portion) and as a result the TCF is dominated by the silicon properties. On the other hand, for higher harmonic QTLM, a larger portion of the total stress field is in Mo/ScAlN/Mo compared to the fundamental mode and therefore the Mo/ScAlN/Mo stack will impact the TCF more prominently. Hence, lower turnover temperature is predicted for these higher order modes.

IV. Fabrication Process

The QTLM-TPoS resonators are fabricated on a relatively thick (16 μm) degenerately Arsenic-doped (~4e19 cm^{-3}) [100] SOI substrate in a five mask process. The sputtered 20% Scandium doped AlN film is 1μm thick and is sandwiched between two 100nm thick layers of Molybdenum.

First, the Mo/ScAlN/Mo stack would be sputtered and the top metal is dry-etched in an SF_6/O_2 plasma to pattern the top electrodes(Fig. 10.a). Then, the ScAlN is wet etched to create access to the bottom electrode (Fig. 10.b). An alternating heated TMAH bath and Sulfuric acid is used for this step. The ScAlN etch rate of 200 nm/min is achieved with this method. Then a thin layer of gold is evaporated on the pads to improve ohmic contact for probing (Fig. 10.b). The resonator body is then formed by plasma etching the full stack of material down to the SOI buried oxide (BOX) layer (Fig. 10.c). Handle layer silicon is then etched from the backside in a deep-reactive-ion-etching tool using Bosch process and the resonator is finally released by wet etching the BOX layer in a buffered oxide etchant (BOE)(Fig. 10.d).

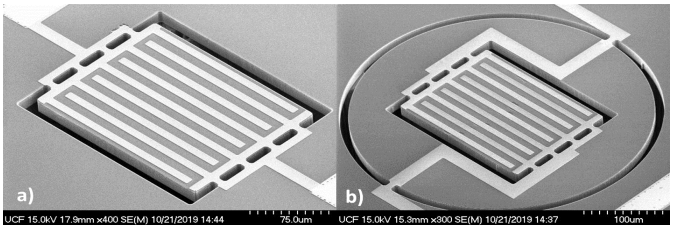

Fig. 11. The SEM image of the fundamental QTLM TPoS resonator without isolation frame (a) and with isolation frame (b).

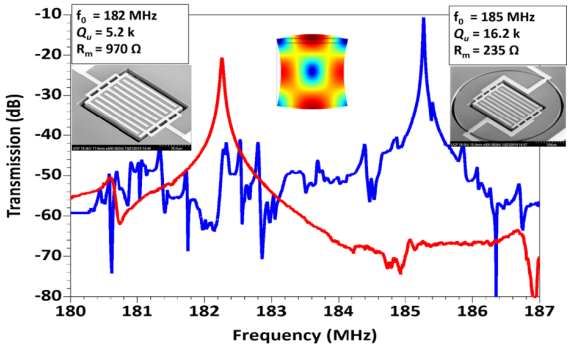

Fig. 12. The measured frequency response in air for the fundamental QTLM TPoS resonator with and without acoustic isolation frame (highest measured Q for both designs). The unloaded quality factor is significantly larger for the devices with isolation frame.

The scanning electron microscopy (SEM) image of the fundamental QTLM TPoS resonator (FP=17μm) with and without isolation frame is shown in Fig. 11.

V. Experimental Results

The fabricated QTLM TPoS resonators are characterized in atmospheric pressure and partial vacuum using a ZNB8 network analyzer and a pair of GSG probes (from FormFactor inc) at ambient temperature. The loaded quality factors are measured from the transmission frequency response and the unloaded quality factors are calculated using the motional resistance of the resonators. The motional resistance is estimated from the insertion loss at the transmission frequency response peak. One port admittance response is also measured and the coupling coefficients are calculated using the measured parallel and series resonance frequencies. The temperature-frequency curves are also measured in a Janis cryogenic vacuum probe station. All the reported plots in this paper are the raw data collected from the network analyzer with 50 Ohm termination impedance (no de-embedding is performed).

TPoS resonators are fabricated on 16 μm thick silicon with finger pitches ranging from 40 μm (lateral-extensional mode) to 17 μm (fundamental QTLM), as well as 9 μm (2nd harmonic QTLM) and 6 μm (3rd harmonic QTLM).

The transmission frequency response for the fundamental QTLM with and without acoustic isolation frame in air is shown in Fig. 12. It is observed that, both quality factor and motional resistance are improved for the device with isolation frame. The measured unloaded quality factor of 16.2 k and

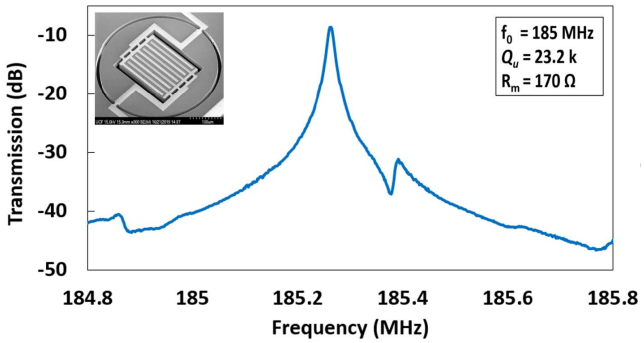

Fig. 13. The measured frequency response of the fundamental QTLM TPoS resonator in partial vacuum. Unloaded quality factor of 23.2 k is measured at 185 MHz for this resonance mode.

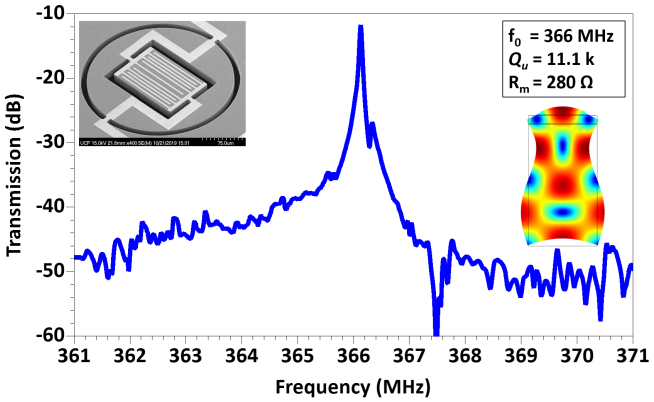

Fig. 14. The measured frequency response for a 2nd harmonic QTLM TPoS resonator in air.

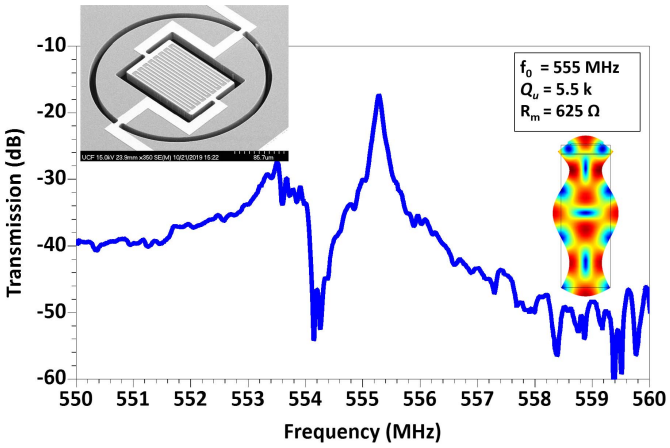

Fig. 15. The measured frequency response for a 3rd-harmonic QTLM TPoS resonator in air.

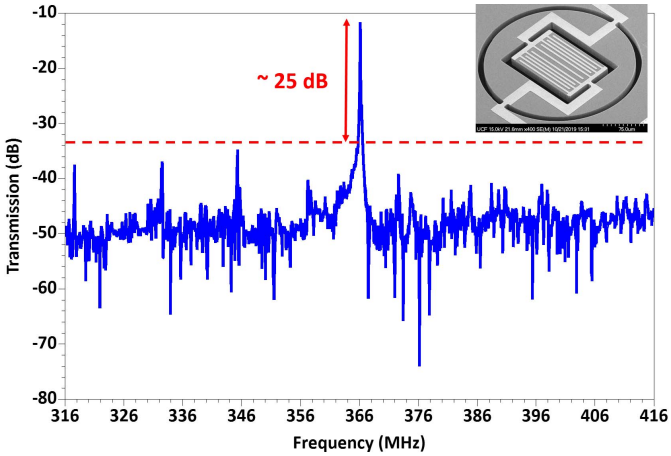

Fig. 16. The wide spectrum frequency response for a second harmonic QTLM TPoS resonator. There are no other strong peak close to this mode which facilitates oscillator applications.

motional resistance of 235 Ohm at 185 MHz for the fundamental QTLM resonator is amongst the best performance reported for any MEMS resonator at this frequency range ($f\times Q\sim 3\times10^{12}$). The measured Q's are in good agreement with the trend predicted by our finite element COMSOL model for anchor quality factor.

As shown in Fig. 13, the transmission frequency response for the fundamental QTLM TPoS resonator is also measured in partial vacuum and an unloaded quality factor of ~23.2 k is measured for this mode shape in vacuum resulting in an $f\times Q\sim 4.3\times10^{12}$. Such a significant Q enhancement in vacuum (more than 40%) is an indication that the quality factor of the resonator is no longer mostly limited by the anchor loss a testament to efficiency of the acoustic isolation frame.

The measured transmission frequency response for the second (FP=9 μm) and third (FP=6 μm) harmonic QTLM TPoS resonators are plotted in Fig. 14 and Fig. 15 respectively. We measure unloaded quality factors of 11.1 k and 5.5 k at 366 MHz and 555 MHz for the second and third harmonic QTLM resonator. The measured unloaded quality factor increased to 12.6 k for the second harmonic QTLM TPoS resonator ($f\times Q\sim4.6\times10^{12}$) in vacuum and the Q for the third-harmonic QTLM improved to 6k in vacuum. The TCF curves are measured for all three harmonics to confirm that the measured peaks are indeed quasi Lamé modes.

TABLE IV
THE MEASURED COUPLING EFFICIENCIES FOR DIFFERENT CLASSES OF TPOS RESONATOR

Mode shape	FP (μm)	Measured K_t^2
Lateral-extensional	40	0.21%
1st harmonic QTLM	17	0.02%
2nd harmonic QTLM	9	0.07%
3rd harmonic QTLM	6	0.1%

A wide spectrum frequency scan is also measured for all three harmonics. We found that there is no strong spurious mode close to these quasi Lamé modes. The second harmonic QTLM spectral response is plotted in Fig. 16. A wide frequency range is deliberately chosen. It is apparent that there are no other strong modes in the vicinity of the QTLM.

The coupling efficiencies of the resonator are calculated from the measured series and parallel frequencies for 5 different resonators in each class and the highest measured

TABLE V

THE MEASURED QUALITY FACTOR FOR THE FUNDAMENTAL QTLM TPoS RESONATOR COMPARED TO A SELECTED PUBLISHED RESULTS IN THE SAME FREQUENCY RANGE

Resonator Type	f_0 (MHz)	Q_{air} (k)	Q_{vac} (k)	R_m Ohm	Resonance mode	Reference
TPoS	185	16.2	23.2	235	Quasi Thickness Lamé	This work
Capacitive	173	9.3	-	18 k	Lamé	[16]
Capacitive	128	12	-	31 k	Lamé	[17]
TPoS	195	9.6	11.5	1.2 k	Radial	[34]
Capacitive	193	8.8	23	-	Radial	[35]

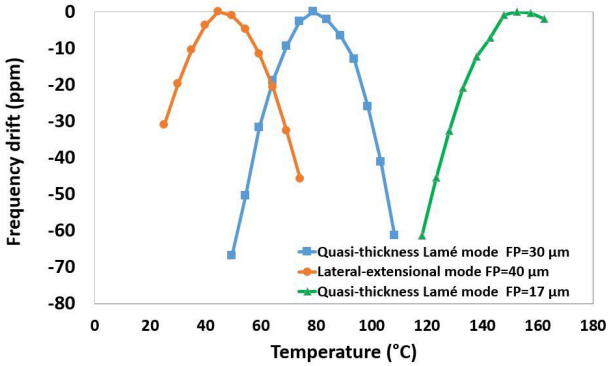

Fig. 17. The measured TCF curves for a lateral-extensional, and two quasi thickness Lamé mode resonators.

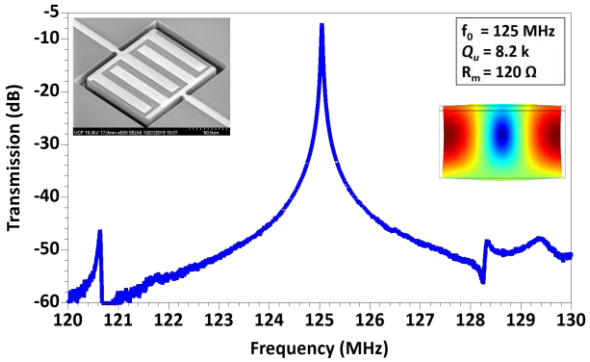

Fig. 18. The measured frequency response for a quasi-thickness Lamé mode resonator with FP = 30 μm.

coupling efficiencies are reported in Table IV. As shown in this table the coupling efficiency improves by actuating higher harmonic QTLM TPoS resonator. The measured coupling efficiencies are in good agreement with the finite element model.

The TCF curves are also measured in vacuum probe station for Lateral extensional and quasi thickness-Lamé mode TPoS resonators. As reported in Fig. 17, the TCF is measured for TPoS resonators with FP=40 μm, FP=30 μm and FP=17 μm and the measured data are in good agreement with the modeled TCF curves. We measure the turnover temperature of 45 °C, 80 °C and 150 °C for these devices respectively. Turnover temperatures reported for QTLM TPoS resonators are the highest turnover temperatures reported for piezoelectric actuated MEMS resonators without any additional over layers.

In Table V, the quality factor of the fundamental QTLM TPoS resonator is compared to several other published results from resonators in the same range of frequencies. To the best of our knowledge, the fundamental QTLM TPoS resonator offers the highest quality factor even compared to highest reported quality factor for capacitive resonators in this range of frequencies.

The best results measured for resonators with FP ranging from 17 μm to 40 μm are compiled in Table VI. The measured transmission frequency response for a resonator with FP=30 μm is shown in Fig.18. As described, in this range

TABLE VI

THE MEASURED RESONANCE CHARACTERIZATION DATA COMPARING THE LE MODE TO QTLM RESONATORS WITH PROPERTIES TRANSITIONING FROM LE TO QTLM FOR A RANGE OF FP

Mode shape	FP (µm)	f_0 (MHz)	Q_{air} (k)	R_m (Ohm)	Turn-Over temperature (°C)
Lateral-extensional	40	95	7.2	80	45
QTLM	30	125	8.2	120	80
QTLM	25	145	7.2	70	95
QTLM	20	170	13.5	225	140
QTLM	17	185	16.2	235	150

the resonator mode shape transitions from QTLM to LE. It is interesting to notice that Q is improved as the device approaches a true TL mode for the 17 μm finger pitch. This is despite the fact that the quality factor is commonly believed to reduce for higher frequency resonators.

VI. CONCLUSION

Fundamental and harmonic quasi thickness-Lamé modes (QTLM) are successfully actuated in the thin-film piezoelectric-on-silicon resonators as the half-wavelength approaches the thickness of the silicon slab. Anchor quality factor in these resonators is shown to significantly improve

by designing an acoustic reflector frame. The resonators are fabricated on a 16 μm thick highly Arsenic-doped silicon layer. A quality factor of 23.2 k (in vacuum) is measured for a fundamental QTLM TPoS resonator at 185 MHz with a measured turnover temperature of above 100 °C which is the highest turnover temperature reported for piezoelectric resonators without the need for any additional silicon oxide over-layer. Quality factors of 12.6 k and 6 k are also measured at 366 MHz and 555 MHz for second- and third-harmonic QTLM TPoS resonators. Very high measured quality factor along with low motional resistance and high turnover temperatures presented in these resonators suggest their suitability for oven-controlled oscillator applications.

ACKNOWLEDGMENT

The authors would like to thank Y. Oshmyansky at Advanced Modular Systems Inc. for his help with the deposition of ScAlN films.

REFERENCES

[1] A. Albarbar, A. Badri, K. Sinha, and A. Starr, "Performance evaluation of MEMS accelerometers," *Measurement*, vol. 42, no. 5, pp. 790–795, 2009.

[2] S. Gong and G. Piazza, "Monolithic multi-frequency wideband RF filters using two-port laterally vibrating lithium niobate MEMS resonators," *J. Microelectromech. Syst.*, vol. 23, no. 5, pp. 1188–1197, Oct. 2014.

[3] R. Abdolvand, H. Lavasani, G. Ho, and F. Ayazi, "Thin-film piezoelectric-on-silicon resonators for high-frequency reference oscillator applications," *IEEE Trans. Ultrason., Ferroelectr., Freq. Control*, vol. 55, no. 12, pp. 2596–2606, Dec. 2008.

[4] J. T. M. Van Beek and R. Puers, "A review of MEMS oscillators for frequency reference and timing applications," *J. Micromech. Microeng.*, vol. 22, no. 1, Jan. 2012, Art. no. 013001.

[5] R. Abdolvand, B. Bahreyni, J. Lee, and F. Nabki, "Micromachined resonators: A review," *Micromachines*, vol. 7, no. 9, p. 160, Sep. 2016.

[6] E. J. Ng, V. A. Hong, Y. Yang, C. H. Ahn, C. L. M. Everhart, and T. W. Kenny, "Temperature dependence of the elastic constants of doped silicon," *J. Microelectromech. Syst.*, vol. 24, no. 3, pp. 730–741, Jun. 2015.

[7] G. Piazza, P. J. Stephanou, and A. P. Pisano, "Piezoelectric aluminum nitride vibrating contour-mode MEMS resonators," *J. Microelectromech. Syst.*, vol. 15, no. 6, pp. 1406–1418, Dec. 2006.

[8] R. T. Smith and F. S. Welsh, "Temperature dependence of the elastic, piezoelectric, and dielectric constants of lithium tantalate and lithium niobate," *J. Appl. Phys.*, vol. 42, no. 6, pp. 2219–2230, May 1971.

[9] M. Shahmohammadi, B. P. Harrington, and R. Abdolvand, "Turnover temperature point in extensional-mode highly doped silicon microresonators," *IEEE Trans. Electron Devices*, vol. 60, no. 3, pp. 1213–1220, Mar. 2013.

[10] R. Tabrizian, G. Casinovi, and F. Ayazi, "Temperature-stable silicon oxide ($SilO_x$) micromechanical resonators," *IEEE Trans. Electron Devices*, vol. 60, no. 8, pp. 2656–2663, Aug. 2013.

[11] W. Pan, P. Soussan, B. Nauwelaers, and H. A. C. Tilmans, "Design and fabrication of a surface micromachined frequency tunable film bulk acoustic resonator with an extended electrostatic tuning range," in *Proc. IEEE Int. Ultrason. Symp. (IUS)*, Rotterdam, The Netherlands, Mar. 2005, pp. 1840–1843.

[12] M. Shahmohammadi, D. Dikbas, B. P. Harrington, and R. Abdolvand, "Passive tuning in lateral-mode thin-film piezoelectric oscillators," in *Proc. Joint Conf. IEEE Int. Freq. Control Eur. Freq. Time Forum (FCS)*, San Francisco, CA, USA, 2011, pp. 1–5.

[13] D. E. Serrano, R. Tabrizian, and F. Ayazi, "Electrostatically tunable piezoelectric-on- silicon micromechanical resonator for real-time clock," *IEEE Trans. Ultrason., Ferroelectr., Freq. Control*, vol. 59, no. 3, pp. 358–365, Mar. 2012.

[14] Z. Wu, A. Peczalski, and M. Rais-Zadeh, "Device-layer ovenization of fused silica micromechanical resonators for temperature-stable operation," in *Proc. Solid-State Sens., Actuators, Microsyst. Workshop*, Hilton Head Island, SC, USA, 2014, pp. 87–90.

[15] J. Lim, K. Choi, H. Kim, T. Jackson, and D. Kenny, "Miniature oven controlled crystal oscillator (OCXO) on a CMOS chip," in *Proc. IEEE Int. Freq. Control Symp. Expo.*, Miami, FL, USA, Jun. 2006, pp. 401–404.

[16] S. A. Bhave, D. Gao, R. Maboudian, and R. T. Howe, "Fully-differential poly-SiC Lamé mode resonator and checkerboard filter," in *Proc. Int. Conf. Micro Electro Mech. Syst.*, Miami Beach, FL, USA, 2005, pp. 223–226.

[17] M. Ziaei-Moayyed, D. Elata, J. Hsieh, J. P. Chen, E. P. Quevy, and R. T. Howe, "Fully differential internal electrostatic transduction of a Lamé-mode resonator," in *Proc. Int. Conf. Micro Electro Mech. Syst.*, 2009, pp. 931–934.

[18] H. Fatemi and R. Abdolvand, "Fracture limit in thin-film piezoelectric-on-substrate resonators: Silicon VS. diamond," in *Proc. Int. Conf. Micro Electro Mech. Syst. (MEMS)*, Taipei, Taiwan, 2013, pp. 461–464.

[19] V. Thakar and M. Rais-Zadeh, "Temperature-compensated piezoelectrically actuated Lamé-mode resonators," in *Proc. Int. Conf. Micro Electro Mech. Syst. (MEMS)*, San Francisco, CA, USA, 2014, pp. 214–217.

[20] A. Prasad, J. Charmet, and A. A. Seshia, "Simultaneous interrogation of high-Q modes in a piezoelectric-on-silicon micromechanical resonator," *Sens. Actuators A, Phys.*, vol. 238, pp. 207–214, 2016.

[21] C. Cassella, G. Chen, Z. Qian, G. Hummel, and M. Rinaldi, "Cross-sectional Lamé mode ladder filters for UHF wideband applications," *IEEE Electron Device Lett.*, vol. 37, no. 5, pp. 681–683, Mar. 2016.

[22] C. Cassella, Y. Hui, Z. Qian, G. Hummel, and M. Rinaldi, "Aluminum nitride cross-sectional Lamé mode resonators," *Microelectromech. Syst.*, vol. 25, no. 2, pp. 275–285, 2016.

[23] M. A. Caro *et al.*, "Piezoelectric coefficients and spontaneous polarization of ScAlN," *J. Phys., Condensed Matter*, vol. 27, no. 24, 2015, Art. no. 245901.

[24] A. Frangi, M. Cremonesi, A. Jaakkola, and T. Pensala, "Analysis of anchor and interface losses in piezoelectric MEMS resonators," *Sens. Actuators A, Phys.*, vol. 190, pp. 127–135, Feb. 2013.

[25] B. Gibson, K. Qalandar, C. Cassella, G. Piazza, and K. L. Foster, "A study on the effects of release area on the quality factor of contour-mode resonators by laser Doppler vibrometry," in *IEEE Trans. Ultrason., Ferroelectr., Freq. Control*, vol. 64, no. 5, pp. 898–904, May 2017.

[26] A. Lozzi, A. De Pastina, L. G. Villanueva, and E. T. Yen, "Release area confinement in Contour mode resonators," in *Proc. IEEE Int. Ultrason. Symp. (IUS)*, Washington, DC, USA, Sep. 2017, pp. 1–4.

[27] C. Cassella, N. Singh, B. W. Soon, and G. Piazza, "Quality factor dependence on the inactive regions in AlN contour-mode resonators," *J. Microelectromech. Syst.*, vol. 24, no. 5, pp. 1575–1582, Oct. 2015.

[28] B. P. Harrington and R. Abdolvand, "In-plane acoustic reflectors for reducing effective anchor loss in lateral–extensional MEMS resonators," *J. Micromech. Microeng.*, vol. 21, no. 8, Aug. 2011, Art. no. 085021.

[29] H. Mansoorzare, S. Moradian, S. Shahraini, J. Gonzales, and R. Abdolvand, "Achieving the intrinsic limit of quality factor in VHF extensional-mode block resonators," in *Proc. Int. Freq. Control Symp. (IFCS)*, 2018, pp. 1–4.

[30] S. Shahraini, H. Fatemi, and R. Abdolvand, "Cross-sectional quasi-Lamé modes in thin-film piezoelectric on silicon resonators," in *Proc. Solid-State Sens., Actuators Microsyst. Workshop*, Hilton Head Island, SC, USA, 2018.

[31] S. Shahraini, H. Fatemi, and R. Abdolvand, "Temperature coefficient of frequency in silicon-based cross-sectional quasi Lamé mode resonator," in *Proc. IEEE Int. Freq. Control Symp. (IFCS)*, Olympic Valley, CA, USA, May 2018, pp. 1–5.

[32] C. M. Lin, T. T. Yen, V. V. Felmetsger, M. A. Hopcroft, J. H. Kuypers, and A. P. Pisano, "Thermally compensated aluminum nitride Lamb wave resonators for high temperature applications," *Appl. Phys. Lett.*, vol. 97, no. 8, 2010, Art. no. 083501.

[33] R. Farraro and R. B. Mclellan, "Temperature dependence of the Young's modulus and shear modulus of pure nickel, platinum, and molybdenum," *Metall. Trans.*, vol. 8, no. 10, pp. 1563–1565, 1977.

[34] S. Shahraini, M. Shahmohammadi, H. Fatemi, and R. Abdolvand, "Side-supported radial-mode thin-film piezoelectric-on-silicon disk resonators," *IEEE Trans. Ultrason., Ferroelectr., Freq. Control*, vol. 66, no. 4, pp. 727–736, Jan. 2019.

[35] J. R. Clark, W. T. Hsu, M. A. Abdelmoneum, and C. T. C. Nguyen, "High-Q UHF micromechanical radial-contour mode disk resonators," *J. Microelectromech. Syst.*, vol. 14, no. 6, pp. 1298–1310, 2005.

Sarah Shahraini (Student Member, IEEE) received the B.Sc. and M.Sc. degrees in electrical engineering from the K. N. Toosi University of Technology, Tehran, Iran, in 2010 and 2012, respectively. She is currently pursuing the Ph.D. degree with the University of Central Florida, Orlando, FL, USA. Her research interests lie in the area of microelectromechanical systems with a special focus on design, fabrication, and characterization of microresonators for stable oscillator, filter, and sensor applications.

Ms. Shahraini was a recipient of the Best Student Paper Award from the 2018 IEEE International Frequency Control Symposium.

Hakhamanesh Mansoorzare (Graduate Student Member, IEEE) received the B.S. degree in electrical engineering from the Sharif University of Technology, Tehran, Iran, in 2016. He is currently pursuing the Ph.D. degree in electrical engineering with the University of Central Florida, Orlando, FL, USA.

He has been working as a Graduate Research Assistant with the Dynamic Microsystems Laboratory. His research interests lie in the area of microelectromechanical systems (MEMS) with a special focus on design, fabrication, and characterization of piezoelectric microresonators for radio frequency circuits and sensors.

Mr. Mansoorzare was a recipient of the Best Student Paper Award in Category 4 from the 2019 Joint Conference of the IEEE International Frequency Control Symposium and European Frequency and Time Forum and upon entering graduate school, he was awarded the ORC Doctoral Fellowship.

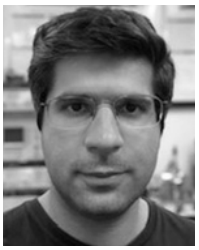

Amirreza Mahigir (Student Member, IEEE) received the B.Sc. and M.Sc. degrees in electrical engineering from the K. N. Toosi University of Technology, Tehran, Iran, in 2009 and 2012, and the Ph.D. degree from the School of Electrical and Computer Engineering, Louisiana State University, Baton Rouge, LA, USA, in 2018. He then joined the University of Central Florida, where he is currently a Post-Doctoral Research Fellow. His research interests are in the area of MEMS-base photonic integrated circuits.

Reza Abdolvand (Senior Member, IEEE) received the Ph.D. degree from the School of Electrical and Computer Engineering, Georgia Institute of Technology, Atlanta, GA, USA, in 2008.

He was an Assistant Professor with the School of Electrical and Computer Engineering, Oklahoma State University, Stillwater, OK, USA. In 2014, he joined the University of Central Florida, Orlando, FL, USA, where he is currently an Associate Professor and the Director of the Dynamic Microsystems Laboratory, Department of Electrical Engineering and Computer Science. He has authored or coauthored two book chapters and more than 70 peer-reviewed journal and conference articles in his field of expertise. He holds 12 U.S. patents. His research interests are in the general area of micro/nanoelectromechanical systems with over 15 years of experience in design, fabrication, and characterization of microresonators with applications in radio frequency circuits and resonant sensors including biosensors.

Dr. Abdolvand was a recipient of the National Aeronautics and Space Administration Patent Application Award in 2009.